Clinical Oncology 33 (2021) 106–116

Contents lists available at ScienceDirect

Clinical Oncology

journal homepage: www.clinicaloncologyonline.net

Overview

# Current Status and Future Direction of Hepatic Radioembolisation

A.A. Alsultan [*], A.J.A.T. Braat [*], M.L.J. Smits [*], M.W. Barentsz [*], R. Bastiaannet [†], R.C.G. Bruijnen [*], B. de Keizer [*], H.W.A.M. de Jong [*], M.G.E.H. Lam [*], M. Maccauro [‡], C. Chiesa [‡]

[*] *Department of Radiology and Nuclear Medicine, University Medical Center Utrecht, Utrecht, the Netherlands*
[†] *Johns Hopkins University School of Medicine, Baltimore, Maryland, USA*
[‡] *Nuclear Medicine Division, Foundation IRCCS National Cancer Institute, Milan, Italy*

## Abstract

Radioembolisation is a locoregional treatment modality for hepatic malignancies. It consists of several stages that are vital to its success, which include a pre-treatment angiographic simulation followed by nuclear medicine imaging, treatment activity choice, treatment procedure and post-treatment imaging. All these stages have seen much advancement over the past decade. Here we aim to provide an overview of the practice of radioembolisation, discuss the limitations of currently applied methods and explore promising developments.


*Key words:* Hepatocellular carcinoma; metastatic colorectal cancer; personalised dosimetry; PET; radioembolisation

## Introduction

Radioembolisation, also known as selective internal radiation therapy or transarterial radioembolisation, is a locoregional treatment modality for hepatic malignancies. It is an angio-guided treatment, where tumours are internally irradiated through injection of radioactive microspheres into the hepatic arterial vasculature. The microspheres lodge and cluster in distal arterioles inside tumours, where they emit high-energy beta-radiation [1]. This procedure relies on the principle that hepatic tumours are almost exclusively supplied by hepatic arteries, whereas healthy liver tissue is mainly supplied by the portal vein [2]. Thus, the radioactive microspheres will predominantly be distributed towards tumoral tissue, relatively sparing healthy liver tissue.

The treatment consists of several stages, starting with a work-up that includes a simulation procedure, in which surrogate particles are injected into a selected liver artery to predict microsphere distribution. Single photon emission computed tomography/computed tomography (SPECT/CT) imaging is then used to visualise these particles and rule out contraindications (e.g. gastrointestinal depositions). The same images can conveniently be used to predict absorbed dose to lesions and non-tumoral tissue, depending on the prescribed therapeutic activity, allowing treatment planning. This is conceptually similar to what is routinely carried out in the radiotherapy department. In a second session, the treatment angiography takes place, in which the beta-radiation-emitting therapeutic microspheres are administered. Post-treatment imaging is then carried out to visualise the microspheres, validating the prediction made with the simulation procedure and allowing the evaluation of the real imparted absorbed dose. Here we aim to provide an overview of the practice of radioembolisation, discuss the limitations of currently applied methods and explore promising developments.

## Radioembolisation Microspheres

There are currently three types of commercially available microsphere (Table 1). These differ in the materials they are made of and the radioisotope they contain. Two products contain the isotope yttrium-90 ($^{90}$Y), a resin microsphere

Author for correspondence: A.A. Alsultan, University Medical Center Utrecht, Heidelberglaan 100, 3584 CX, Utrecht, the Netherlands. Tel: +31-887574675.
*E-mail address:* A.A.N.Alsultan@umcutrecht.nl (A.A. Alsultan).

https://doi.org/10.1016/j.clon.2020.12.003

**Table 1**
Microsphere characteristics

| | SIR-Spheres® | TheraSphere® | QuiremSpheres® |
|---|---|---|---|
| Radioisotope | Yttrium-90 | Yttrium-90 | Holmium-166 |
| Half-life (h) | 64.1 | 64.1 | 26.8 h |
| Main emitted radiation | Beta | Beta | Beta and gamma |
| Mean (maximum) tissue penetration (mm) | 2.5 (11) | 2.5 (11) | 2.5 (8.4) |
| Visualisation method | Bremsstrahlung-SPECT<br>Yttrium-90 PET | Bremsstrahlung-SPECT<br>Yttrium-90 PET | MRI<br>SPECT |
| Material | Resin | Glass | Poly-L-lactic acid |
| Microsphere size (μm; range) | 32.5 (20–60) | 25 (20–30) | 30 (25–35) |
| Specific activity per sphere (Bq) | 40–70 | 4354*, 1539†, 544‡ | 200–400 |
| Millions of spheres in a typical administration | 20–40 | 1.7† 4.8‡ | 12–24 |
| Embolic effect | Moderate | Low | Moderate |
| Treatment planning method indicated in product leaflet. | BSA (two compartment) | Mono-compartment | Mono-compartment |

BSA, body surface area; MRI, magnetic resonance imaging; PET, positron emission tomography; SPECT, single photon emission computed tomography.
* Measured, at the reference date [6].
† Four days after the reference time.
‡ Eight days after the reference time.

(SIR-Spheres®, Sirtex Medical Ltd, Woburn, MA, United States) and a glass microsphere (TheraSphere®, Boston Scientific, Marlborough, MA, United States) [3,4]. The third type are poly-L-lactic acid microspheres and contain holmium-166 ($^{166}$Ho) (QuiremSpheres®, Quirem Medical B.V., Deventer, the Netherlands) [5].

Both $^{166}$Ho and $^{90}$Y emit beta-radiation with a comparable energy level. Differences between the microspheres include a higher specific activity per sphere in glass microspheres compared with resin and holmium microspheres. This results in a lower number of injected glass particles (Table 1), which allows for the treatment of small volumes [7], as well as the treatment of main portal vein thrombosis (PVT) [8]. It also has radiobiological implications, for instance, a lower embolic effect compared with the moderate embolic effect of the other two microspheres [9].

## Patient Selection

The most common indication for radioembolisation in Europe is hepatocellular carcinoma (HCC), followed by metastatic colorectal carcinoma (mCRC) [10]. In unilobar HCC, radioembolisation can be applied with curative intent in a limited number of cases, or as a bridge to hepatic resection (i.e. radiation lobectomy), when it is applied to induce hypertrophy of the future liver remnant while maintaining tumour control [11,12]. In bilobar or multifocal unilobar HCC, radioembolisation is mostly applied with palliative intent (Figure 1) [13]. For mCRC patients, the European Society for Medical Oncology consensus guideline states that radioembolisation should be considered for patients with liver-limited disease after exhausting the available systemic options, as a salvage treatment (Figure 2) [14].

There are several relative and absolute contraindications for radioembolisation (Table 2) [15,16]. A pre-treatment work-up includes evaluation of clinical performance status, haematological and biochemical status, assessment of the anatomy using CT-angiography/magnetic resonance angiography, and in specific situations molecular imaging with SPECT/CT (e.g. hepatobiliary scintigraphy to assess liver function) or positron emission tomography/computed tomography (PET/CT; e.g. $^{18}$FDG-PET/CT to assess extrahepatic disease).

Whether the presence of extrahepatic disease should be permitted is a matter of debate, on the grounds that extrahepatic disease would go untreated in a locoregional treatment such as radioembolisation. In the current guidelines for HCC and mCRC, radioembolisation is recommended in cases with liver-dominant disease [14,17]. In randomised controlled trials (RCT) on HCC, the presence of extrahepatic disease was mostly excluded [18–20], whereas some RCTs in mCRC would include patients with limited extrahepatic disease (i.e. lymph node and lung metastases) [21].

## Pre-treatment Work-up

The distribution of microspheres is mainly determined by catheter position, vascular anatomy and blood flow dynamics. Thus, prior to the actual treatment, a simulation angiography is carried out using a surrogate for $^{90}$Y-microspheres in the form of gamma-radiation-emitting technetium-99m ($^{99m}$Tc) macroaggregated albumin (MAA) (multiple suppliers available; ±150 MBq) [22]. For the simulation of $^{166}$Ho radioembolisation, a small amount of actual $^{166}$Ho-microspheres (QuiremScout®; Terumo, Tokyo, Japan; ±250 MBq; ±2–3 million microspheres) can be used instead of $^{99m}$Tc-MAA. The surrogate particles are injected into the position selected for the actual intra-arterial treatment. A SPECT/CT scan is carried out shortly afterwards to assess the predicted distribution of microspheres. Technical contraindications, such as extrahepatic deposition of activity or excessive lung shunting, can be ruled out using this procedure.

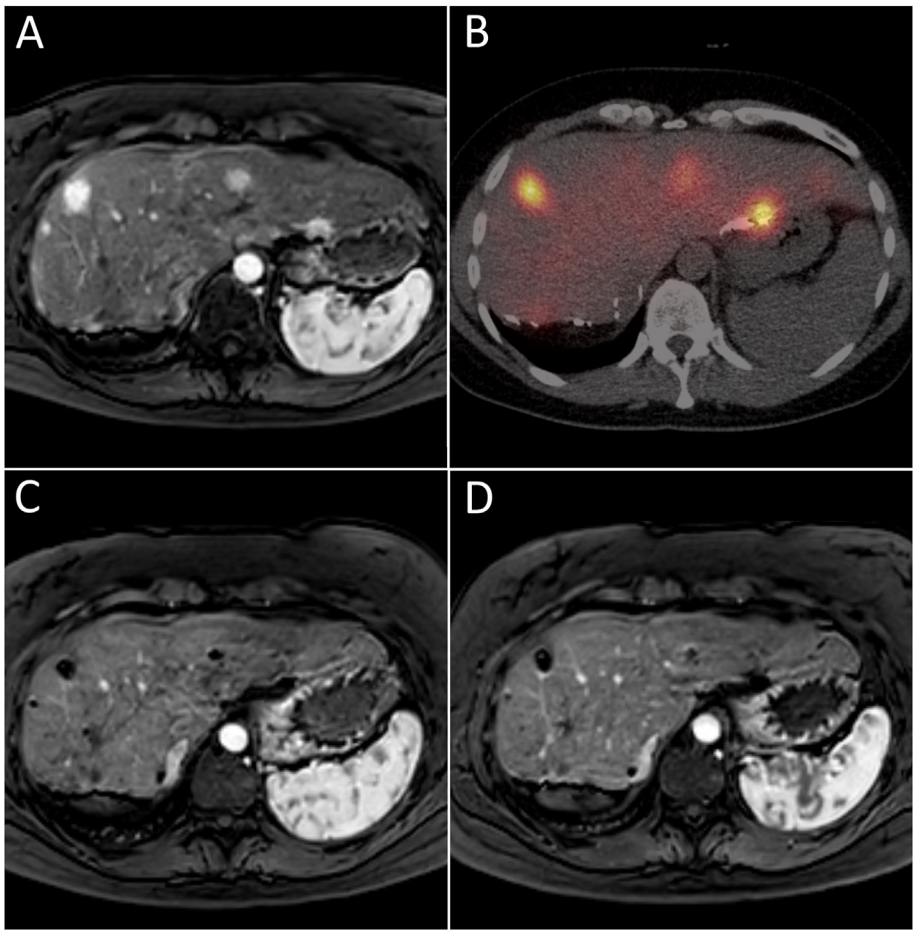


**Fig 1.** An example of a patient with a multifocal recurrent hepatocellular carcinoma (HCC), treated with $^{166}$Ho-microspheres. (A) Magnetic resonance imaging (MRI) at baseline showing multiple hypervascular lesions in the remnant liver after right-sided hemi-hepatectomy, the largest in segment IV. (B) Post-treatment $^{166}$Ho single photon emission computed tomography/computed tomography (SPECT/CT), showing good targeting of the HCC lesions. (C) MRI 1 day after treatment demonstrating depositions of microspheres inside the tumour in black. (D) MRI at 3 months post-treatment, showing avascular lesions.

Extrahepatic deposition occasionally occurs in organs with a close vascular relationship to the liver. Vessels such as the gastroduodenal artery, right gastric artery or cystic artery may arise from arteries that are targeted in radioembolisation [23]. Extrahepatic deposition of microspheres can potentially lead to gastrointestinal ulceration [15]. For this reason, such depositions are an absolute treatment contraindication [8], unless this situation is solved. When extrahepatic deposition is detected on the pre-treatment simulation SPECT/CT (or alternatively on cone beam CT during angiography), the culprit (non-target) vessel should be identified. The extrahepatic collateral flow can then be mitigated by embolisation of the culprit vessel using coils, or alternatively, the injection position can be moved to a distal location beyond the origin of the culprit vessel. In 96% of the cases, patients are deemed eligible for treatment after a second treatment simulation [24]. Another method, known as 'skeletonisation' (i.e. coil embolisation of all side branches of the hepatic artery), which used to be common practice, is no longer considered necessary, partly due to the use of injection positions that are located distally in the right and/or left hepatic arteries instead of a single proximal location in the proper hepatic artery [10].

Arteriovenous anastomoses, present in the hepatic tumours or parenchyma, allow microspheres to shunt towards the lungs through the venous circulation, which may lead to radiation pneumonitis [25]. Thus, excessive lung shunting is considered a contraindication. Lung shunting mostly occurs in HCC and is uncommon in other tumour types [26]. The currently applied safety threshold for lung shunting indicated by producers, based on planar imaging, is 30 Gy and up to 50 Gy cumulatively after multiple treatments for glass $^{90}$Y- and $^{166}$Ho-microspheres, and 20% lung shunt fraction for resin $^{90}$Y-microspheres [3].

However, we do have strong indications that this method largely overestimates lung shunt fraction, both for the scan type used (planar instead of tomographic), and, above all, because MAA have different morphology and size compared with therapeutic microspheres [27].

## Treatment Planning and Post-treatment Imaging

The dual vascularisation principle implies that most intra-arterially administered microspheres will accumulate

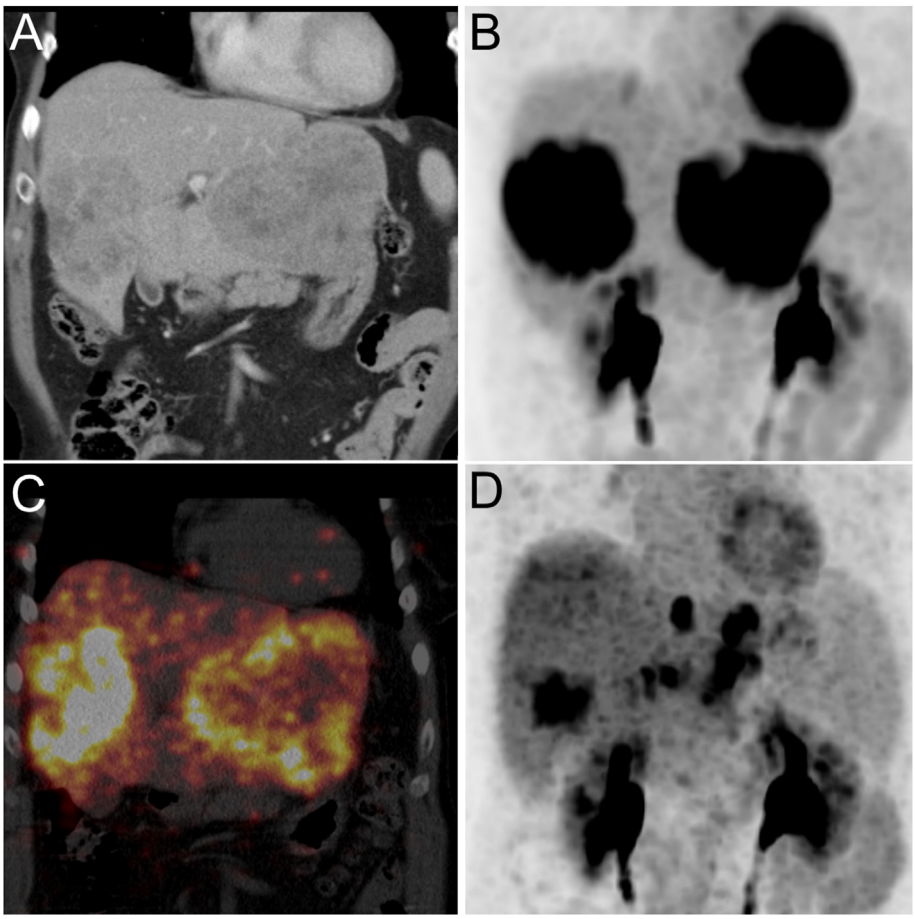


**Fig 2.** Example of a glass yttrium-90 ($^{90}$Y) radioembolisation of metastatic colorectal carcinoma in salvage setting. (A, B) Baseline portal-phase computed tomography scan and $^{18}$FDG-positron emission tomography ($^{18}$FDG-PET) of a patient with two large metastases in the left and right liver lobes (10.3 and 9.2 cm). (C) Post-treatment $^{90}$Y-PET showing favourable tumour targeting, post-treatment dosimetry revealed a tumour absorbed dose of 114 Gy to the lesion in the left lobe and 197 Gy to the lesion in the right lobe. (D) Three-month follow-up $^{18}$FDG-PET showing partial response of the two treated lesions, as well as three small new hepatic lesions in the left lobe.

inside the tumour. However, this is not always the case, as the intrahepatic distribution difference, expressed by the tumour-to-non-tumour ratio (T/N), can vary greatly between patients. This ratio is dependent on many factors, e.g. tumour type, tumour vascularity, vascular invasion, selected injection position. A high T/N ratio allows for a relatively high tumour dose while maintaining a relatively low healthy liver absorbed dose.

Treatment activity planning methods differ depending on the type of microspheres used. Most commonly used are the body surface area (BSA)-based method for resin microspheres and the Medical Internal Radiation Dose

**Table 2**
Relative and absolute contraindications for radioembolisation

| Criterion | Contraindications | |
|---|---|---|
| | Relative | Absolute |
| Clinical condition | | ECOG performance score >2 |
| Life expectancy | | <3 months |
| Organ function | Mild to moderate laboratory abnormalities | Critical renal or bone marrow failure |
| Hepatic function | Cirrhosis (Child-Pugh score > B7), serum bilirubin >34.2 μmol/l (i.e. 2 mg/dl) | Uncompensated hepatic failure, active hepatitis |
| Biliary system | Biliary stents/bile duct abnormalities | Cholangitis |
| Macrovascular invasion | | Main branch portal vein thrombosis, hepatic vein invasion |
| Technical aspects | | Excessive lung shunt, uncorrectable gastrointestinal deposition of microspheres. |

ECOG, Eastern Cooperative Oncology Group.

(MIRD) 'mono-compartment' method for glass and holmium microspheres. The BSA method was developed to curtail the high toxicity that was observed in early clinical studies [28]. The treatment activity is calculated using a formula that takes the fractional tumour involvement into account, and the BSA as a surrogate for liver size [3]. A large study in 680 patients that compared the BSA method with the previously used 'empirical' method found a lower rate of toxicity in the BSA cohort [29]. It also reported lower median prescribed activities in the BSA cohort compared with the 'empirical' cohort, 1.6 ± 0.5 GBq versus 2.0 ± 0.4 GBq, respectively. It is interesting to note that the actually administered activity was even lower (i.e. 1.1 ± 0.6 GBq), as in 98% of cases ($n = 491$) it was lowered even further based on physicians' discretion (1.6 ± 0.5 GBq calculated with BSA method, 1.2 ± 0.6 GBq physician's prescription).

The MIRD 'mono-compartment' activity calculation method is based on a desired average absorbed dose to the treated part of the liver [4,5]. An average absorbed dose ranging from 80 to 150 Gy is recommended for glass and a fixed 60 Gy absorbed dose for holmium microspheres. The treated 'mono-compartment' encompasses both tumour and non-tumorous tissue and does not differentiate between the two. However, these two recommended absorbed dose limits are markedly different. As for glass spheres, the recommended dose range is more broad. Furthermore, the target is more ambiguous, as the instruction for user reports 'dto liver', without specifying if the indication refers to the treated portion or to the whole liver.

For $^{166}$Ho spheres, the limit was determined with an escalation study where 20, 40, 60, 80 Gy were imparted to whole liver [30]. Toxicity was observed at the last step; therefore 60 Gy was chosen as the safety limit. This value initially referred to the treated portion in case of lobar or segmental treatment, whereas in the new $^{166}$Ho indications, it refers to the whole liver, no matter if the treatment is lobar. This means that a smaller treated region can tolerate a proportionally higher absorbed dose, in agreement with the basic radiobiology of parallel organs, the well-known volume effect in external beam, and with the most recent experimental findings in radioembolisation [31,32].

The main goal of these methods is to ensure treatment safety; however, the different microsphere concentration in tumour and non-tumoral tissue is not taken into consideration. The absorbed doses in these two compartments vary significantly among patients, mostly resulting in underdosing patients to sustain overall safety [33–35]. Furthermore, BSA was later shown to be a poor surrogate for liver volume, leading to underdosing in patients with large livers relative to their BSA and overdosing in relatively small livers (Figure 3) [36].

An alternative method for treatment planning is the 'multi-compartment' method. The first developed method in this direction is known as the partition model. This model takes three compartments into consideration: tumour, non-tumorous liver and lungs. Treatment planning aims at maximising the absorbed dose to the tumour while staying below the safety thresholds for healthy liver and the lungs [37]. The advantage of the partition model in comparison with the previously mentioned planning method is that it differentiates between absorbed dose to target and non-target tissue, as requested by the EU Directive 2013/59. One limitation is that the tumour absorbed dose is averaged over many lesions. More advanced methods evaluate absorbed dose for any single lesion. Furthermore, multi-compartment methods require threshold validations for both safety and efficacy. Clinical studies have shown large variations in these thresholds between tumour types and the used microspheres [16,38–40]. This subject, called dosimetry, will be discussed in the next section.

The weak point of treatment planning is the limited accuracy of absorbed dose prediction obtained with $^{99m}$Tc MAA SPECT/CT, especially with regards to small lesions. The 95% confidence interval of the differences between predicted and actual lesion absorbed dose is as wide as some hundreds of Grays [41–45]. Such large uncertainties clearly pose limitations to the prognostic accuracy on lesion response. This mismatch depends, amongst others, on the different repositioning of catheter tip position between the

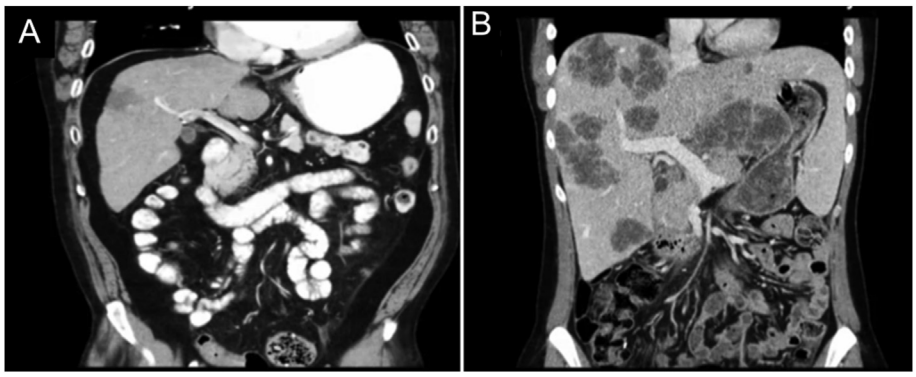


**Fig 3.** An example of two patients treated for metastatic colorectal carcinoma with resin yttrium-90 ($^{90}$Y)-microspheres using the body surface area (BSA) treatment planning method. Using the BSA method both patients received a similar amount of activity. For patient A, who has a small liver with a limited tumour volume, this resulted in an absorbed dose that was too high and resulted in radioembolisation-induced liver disease within 3 months post-treatment. In contrast, patient B, who has a large liver relative to their BSA with a large tumour volume, was underdosed and had disease progression within 3 months.

simulation and the therapy sessions, especially in the proximity of an arterial bifurcation [46,47]. However, the problem persists if repositioning is accurate [48]. Many other factors may be responsible for this mismatch too, including the use of two different kinds of particle in the two sessions, and a different number. The use of the same $^{166}$Ho particle for the two sessions significantly reduced the prediction uncertainty on lesion absorbed dose [45,49]. As the prediction on non-tumoral liver tissue is less subject to uncertainty than lesions, another improvement in planning is using the dose–toxicity relationship in order to deliver the maximum tolerable absorbed dose [45].

The two isotopes used in radioembolisation can be imaged in several ways (Table 1). Post-treatment imaging has its rationale in the often-reported differences between the predicted and the actual therapeutic biodistribution. It can be used either to visually assess the intra- and extra-hepatic distribution of microspheres or for quantitative verification (dosimetry). The visual check allows prompt medical action in case of inadvertent deposition in the gastro-enteric tract, whereas post-treatment dosimetry is used to evaluate treatment success, validating the prediction made using the pre-treatment simulation. Suboptimal absorbed dose distribution can be corrected with a second administration, without waiting for disease recurrence [50].

## Treatment Outcomes in Relation to Absorbed Dose

SPECT/CT images can be conveniently used to predict the absorbed dose to lesions and to the heathy tissue depending on the prescribed activity for therapy. This allows therapy to be optimised and personalised (treatment planning), as required by the EU Directive 2013/59 for nuclear medicine therapy, as well as external beam radiotherapy [51]. In the era of personalised medicine, we expect that such an option could significantly improve the clinical outcome of radioembolisation.

Radioembolisation is a generally well-tolerated treatment, which may be accompanied by mostly mild side-effects, including abdominal pain, nausea, vomiting, fatigue and fever, occurring within 4–6 weeks after treatment [15,52]. Side-effects almost always resolve without further treatment. Interestingly, in HCC patients with PVT (Barcelona Criteria for Liver Cancer [BCLC] C), the standard of care treatment with sorafenib produces more severe side-effects, with a more marked worsening of quality of life [53]. There are some more severe complications associated with radioembolisation, of which radioembolisation-induced liver disease (REILD) is the most severe and potentially fatal. In general, hyperbilirubinemia, hypoalbuminemia, jaundice and ascites as signs of liver failure are regarded as indicative of REILD, unless explained by biliary obstruction or disease progression [54]. The severity of the toxicity ranges from minor changes in biochemical markers, to REILD necessitating invasive medical treatment and fatal REILD. The exact incidence of toxicity after radioembolisation is controversial as different authors adopted different end point definitions. For instance, according to Kennedy *et al.* [29], REILD incidence was estimated to be 1–3% in most practices, whereas Strigari *et al.* reported CTCAE v4 toxicity of 32% $\geq$ grade 2, 21% $\geq$ grade 3, 11% $\geq$ grade 4 (death related to treatment) after resin $^{90}$Y-microspheres for HCC planned with the BSA method [55]. They included any kind of liver toxicity, imputable both to treatment and to the natural history of disease itself (i.e. tumour and cirrhosis). REILD is associated with the baseline liver condition, indicated by the Child-Pugh score for cirrhosis. In total, 8/9 (89%) Child-Pugh B7 patients showed liver decompensation after standard administration of glass $^{90}$Y-microspheres [56], whereas in a Child-Pugh A cohort planned with mixed criteria (standard indication and personalised dosimetry) it was 11%. Baseline bilirubin >1.1 mg/dl and absorbed dose to the whole non-tumoral liver were ascertained as risk factors for treatment-related liver decompensation, both with glass and resin $^{90}$Y-microspheres [57,58]. Therefore, a proper patient selection and treatment planning are mandatory to limit the toxicity rate.

### *Hepatocellular Carcinoma*

In HCC, according to the modified BCLC scheme, radioembolisation is mainly positioned for intermediate (BCLC B) and advanced (BCLC C) patients [52]. Several relationships between absorbed dose and tumour response were found in HCC patients treated with glass $^{90}$Y-radioembolisation using post-treatment dosimetry [59]. One study found significantly higher tumour absorbed doses in responders (per mRECIST) compared with non-responders (225 Gy versus 83 Gy) [60]. Furthermore, all tumours that received a tumour absorbed dose >200 Gy had an objective response. Another study found a response rate of 89.7% in patients with tumour absorbed doses $\geq$205 Gy on $^{99m}$Tc-MAA compared with 9.1% in tumour doses <205 Gy [51]. Moreover, a dose-toxicity relationship was shown in HCC treated with glass $^{90}$Y-microspheres in two studies, proposing comparable safety thresholds of up to 90 Gy in the healthy liver tissue [51,58].

Initial results, confirming improved overall survival in HCC by dosimetric treatment planning, are available in a study on sequential cohorts and even in a prospective randomised trial. The first study reported that median overall survival of HCC Child A patients with PVT was 12 months versus 8 months for the cohort planned using dosimetry versus the standard indication of 80–150 Gy, albeit non-significant $P = 0.067$ [61]. Lesion volumes were not significantly different between the two PVT cohorts. On the other hand, for the two cohorts without PVT, lesions were significantly larger in the cohort treated using dosimetry. Despite that, median overall survival was preserved due to dosimetry, with a non-significant difference of 15 (dosimetry) versus 17 months (standard indication).

A RCT comparing resin $^{90}$Y-radioembolisation with sorafenib in advanced HCC (SARAH trial), showed an improvement in tumour response and a decrease in adverse events [18]. However, they failed to show improvement in overall or progression-free survival. It is noteworthy that

the BSA method was used, which is prone to underdosing [36].

A recently published post-hoc analysis of the SARAH trial showed improved overall survival and response in patients with tumour absorbed doses >100 Gy versus an absorbed dose <100 Gy (median overall survival 14.1 months versus 6.1 months; $P = 0.001$) [62]. Furthermore, pre-treatment $^{99m}$Tc-MAA SPECT/CT dosimetry was an independent predictor of prolonged survival, suggesting that with improved treatment planning methods, a survival benefit might have been predicted and achieved [63]. The impact of pre-treatment dosimetry in HCC was studied in a recently completed RCT on glass $^{90}$Y-microspheres (DOSISPHERE-01), which is a milestone in the progress of dosimetry in radioembolisation and in nuclear medicine therapy. Authors compared a prospective personalised dosimetry approach (multi-compartment, >205 Gy to index lesion) versus standard indication (mono-compartment dosimetry, 120 Gy average absorbed dose in the target volume). Prescribing the therapeutic activity according to pre-treatment dosimetry showed an improved response rate at 3 months after treatment (response rate: 79% versus 43%, $P = 0.0062$), as well as improved overall survival in the personalised dosimetry group (26.7 months versus 10.6 months, $P = 0.0096$) [64]. For treatment of HCC with glass $^{90}$Y-microspheres, an international panel of experts now recommends >200 Gy as a threshold for tumour absorbed dose to achieve response using pre-treatment dosimetry on $^{99m}$Tc-MAA SPECT/CT images [16].

It is interesting to note that such improved outcomes based on $^{99m}$Tc-MAA SPECT/CT dosimetry were obtained despite the mentioned mismatch between pre- and post-treatment absorbed dose evaluation. This can be understood considering that such differences are zero on the average. Therefore, we have an average outcome improvement thanks to pre-treatment dosimetry if we consider average properties of a studied cohort (like median overall survival). On the contrary, we may have unexpected outcomes in individual patients when the actual lesion absorbed dose deviates from the prediction.

*Metastatic Colorectal Cancer*

In mCRC, dose-response relationships have also been established in mCRC treatment with resin $^{90}$Y-microspheres, and more recently in $^{166}$Ho- and glass $^{90}$Y-microspheres. A conservative estimate for the minimum absorbed dose to reach metabolic response (50% reduction in total lesion glycolysis on $^{18}$F-FDG-PET) was 40–60 Gy using resin $^{90}$Y-microspheres, calculated on post-treatment $^{90}$Y PET imaging [38]. In $^{166}$Ho treatment of mCRC, the mean tumour absorbed dose was higher by 84% in responders versus patients with progressive disease. Furthermore, patients receiving tumour absorbed doses >90 Gy had a significantly higher overall survival versus patients with tumour absorbed doses <90 Gy [39]. In treatment with glass $^{90}$Y-microspheres, a tumour absorbed dose ≥183 Gy on post-treatment dosimetry predicted a metabolic tumour response at 3 months with 97% specificity. Furthermore, the mean tumour absorbed dose was higher by 111% in responders versus patients with progressive disease ($P = 0.02$) [65].

Resin $^{90}$Y-radioembolisation was investigated as a first-line treatment for mCRC in three large RCTs, the SIRFLOX, FOXFIRE and FOXFIRE Global [66]. These trials were designed to assess whether radioembolisation combined with first-line chemotherapy (FOLFOX) can improve overall survival compared with chemotherapy alone. Although an improved objective response rate (75.8% versus 63.7%, $P = 0.001$) and liver-specific progression-free survival (hazard ratio 0.90, 95% confidence interval 0.79–1.02, $P = 0.108$) were reported, an additional overall survival benefit was not shown. Treatment planning was carried out using the BSA method, modified to reduce the dose even further based on increasing lung shunt fractions and fractional liver involvement. Currently, there is one large RCT ongoing in glass $^{90}$Y-radioembolisation of mCRC (EPOCH) as a second-line treatment versus chemotherapy [67]. However, the MIRD 'mono-compartment' is used for treatment planning. There are currently no RCTs in the treatment of mCRC using prospective dosimetry.

## Future Perspectives

Currently used treatment planning methods (BSA and MIRD) in radioembolisation are the most significant limitations of this treatment and the currently published outcomes in literature. The lack of dosimetric treatment planning was advocated as one of the reasons of the failure of these large phase III trials on mCRC [68], as well as the SARAH study on HCC. Understanding dose-response relationships and the use of a more accurate simulator than MAA can lead to improved planning methods that permit a truly individualised approach. With this new device, the implementation of 'multi-compartment'-based planning methods adds a new dimension to patient selection, allowing for exclusion of patients that are not expected to benefit from the treatment based on intrahepatic microsphere distribution on scout dose SPECT/CT. In contrast to the current practice, in which patients can receive radioembolisation if the $^{99m}$Tc-MAA scan shows no extrahepatic deposition (about 90–95% of patients), pre-treatment dosimetry will be added to the selection process. A good probability of response requires that the predicted tumour dose reaches a pre-defined tumoricidal threshold, with an expected parenchyma dose staying below a pre-defined safety threshold. As discussed in the previous section, these thresholds vary between tumour types and dimension, and therapeutic particle used.

Once treatment planning has been matured, only then can the potential role of radioembolisation in earlier lines of disease treatment be properly studied. There are still several clinical trials underway that use BSA and 'mono-compartment' MIRD dosimetry (SIRCCA-trial: resin $^{90}$Y-radioembolisation followed by cisplatin + gemcitabine (CIS-GEM) versus CIS-GEM as a first-line treatment for unresectable intrahepatic cholangiocarcinoma (ICC); EPOCH-trial: glass $^{90}$Y-radioembolisation as a second-line treatment for mCRC followed by resumption of

chemotherapy versus chemotherapy alone). Unfortunately, these studies suffer from the same limitations as previous phase III trials. These trials will need to be evaluated in the light of proper pre- and post-treatment dosimetry. Together with placement in earlier treatment lines, radioembolisation can also be studied as a combined treatment with other embolic therapies, such as trans-arterial chemoembolisation (DEBIR$^{90}$Y-trial) or locoregional ablative therapies (HORA EST-trial). The leading-edge research should combine immunotherapy and radioembolisation, the latter used either as a trigger of immune response (low tumour absorbed dose required) or as additional treatment (high tumour absorbed dose).

The next step in improving radioembolisation treatment planning may lie in voxel-based dosimetry. Simply put, a voxel is a three-dimensional pixel, i.e. the smallest measured spatial unit. Using voxel-based dosimetry one can extract information on the heterogeneity of the distribution of microspheres within each compartment, as ordinarily carried out in external beam radiotherapy planning. This may be a step forward with respect to 'multi-compartment' MIRD dosimetry, in which the absorbed dose is averaged over each compartment [28]. Metrics such as the $D_{70}$ (i.e. lowest absorbed dose to 70% of the volume) and $V_{100}$ (i.e. percentage of the volume with an absorbed dose above 100 Gy) are examples of spatially dependent parameters that may prove to be better at demonstrating dose-effect [56,69]. Unfortunately, such proof has not yet been obtained, and the mean absorbed dose in each compartment is still a good parameter [56,70].

A noteworthy advance in the field of radioembolisation comes in the development of specialised imaging systems. Traditional C-arm devices contain an X-ray tube and detector and can convey anatomical information in real-time but lack the ability to visualise radioactive particles. A novel device that integrates a gamma camera with the X-ray system may overcome this limitation and is currently in development [71,72]. In radioembolisation treatment this technology can visualise the distribution of microspheres as they are being injected, allowing physicians to adjust during treatment when necessary.

## Conclusion

Radioembolisation is a safe and effective treatment for hepatic malignancies. RCTs failed to show survival benefit over current systemic treatments, partly due to imperfect treatment planning methods. Improved and personalised treatment planning methods, based on distinct prediction of absorbed dose to tumour and non-tumoral tissue, is under development and recently showed promising results in terms of improved clinical outcome.

## Conflicts of interest

A.A. Alsultan reports personal fees from Boston Scientific, outside the submitted work. M.G.E.H. Lam reports grants, personal fees and non-financial support from Boston Scientific, personal fees and non-financial support from Terumo, personal fees, non-financial support and other from Quirem Medical, outside the submitted work. M. Maccauro reports personal fees from Boston Scientific, personal fees from Terumo, outside the submitted work. C. Chiesa reports grants and personal fees from Boston Scientific, personal fees from Terumo, personal fees from Alfasigma, outside the submitted work. M.L.J. Smits and A.J.A.T. Braat report personal fees from Boston Scientific, personal fees from Terumo, personal fees from SirTex, outside the submitted work.

## Funding

This research did not receive any specific grant from funding agencies in the public, commercial, or not-for-profit sectors. ORCID:0000-0003-4236-1376.

## References

[1] Kennedy A. Radioembolization of hepatic tumors. *J Gastrointest Oncol* 2014;5:178–189. https://doi.org/10.3978/j.issn.2078-6891.2014.037.

[2] Riemenschneider T, Ruf C, Kratzsch HC, Ziegler M, Späth G. Arterial, portal or combined arterio-portal regional chemotherapy in experimental liver tumours? *J Cancer Res Clin Oncol* 1992;118:597–600. https://doi.org/10.1007/BF01211803.

[3] [internet]*SirSphere® Sirtex package insert*. Sirtex Medical, Ltd; 2017. p. 1–3 [cited 10 July 2020] n.d.

[4] TheraSphere® Yttrium-90 Glass microspheres [package insert]. Biocompatibles UK Ltd. Rev. 14. n.d.

[5] Quiremspheres® Holmium-166 microspheres instructions for use [internet]. *Quirem Med* 2020:1–5 [cited 10 July 2020] n.d.

[6] Pasciak AS, Abiola G, Liddell RP, Crookston N, Besharati S, Donahue D, *et al*. The number of microspheres in Y90 radioembolization directly affects normal tissue radiation exposure. *Eur J Nucl Med Mol Imag* 2020;47:816–827. https://doi.org/10.1007/s00259-019-04588-x.

[7] Salem R, Thurston KG. Radioembolization with 90yttrium microspheres: a state-of-the-art brachytherapy treatment for primary and secondary liver malignancies - Part 1: Technical and methodologic considerations. *J Vasc Interv Radiol* 2006;17:1251–1278. https://doi.org/10.1097/01.RVI.0000233785.75257.9A.

[8] Giammarile F, Bodei L, Chiesa C, Flux G, Forrer F, Kraeber-Bodere F, *et al*. EANM procedure guideline for the treatment of liver cancer and liver metastases with intra-arterial radioactive compounds. *Eur J Nucl Med Mol Imag* 2011;38:1393–1406. https://doi.org/10.1007/s00259-011-1812-2.

[9] Sato K, Lewandowski RJ, Bui JT, Omary R, Hunter RD, Kulik L, *et al*. Treatment of unresectable primary and metastatic liver cancer with yttrium-90 microspheres (TheraSphere®): assessment of hepatic arterial embolization. *Cardiovasc Intervent Radiol* 2006;29:522–529. https://doi.org/10.1007/s00270-005-0171-4.

[10] Reinders MTM, Mees E, Powerski MJ, Bruijnen RCG, van den Bosch MAAJ, Lam MGEH, *et al*. Radioembolisation in Europe: a survey amongst CIRSE members. *Cardiovasc Intervent Radiol* 2018;41:1579–1589. https://doi.org/10.1007/s00270-018-1982-4.

[11] Lewandowski RJ, Donahue L, Chokechanachaisakul A, Kulik L, Mouli S, Caicedo J, *et al*. $^{90}$ Y radiation lobectomy: outcomes

following surgical resection in patients with hepatic tumors and small future liver remnant volumes. *J Surg Oncol* 2016; 114:99–105. https://doi.org/10.1002/jso.24269.

[12] Lewandowski RJ, Gabr A, Abouchaleh N, Ali R, Al Asadi A, Mora RA, *et al*. Radiation segmentectomy: potential curative therapy for early hepatocellular carcinoma. *Radiology* 2018; 287:1050–1058. https://doi.org/10.1148/radiol.2018171768.

[13] Salem R, Gordon AC, Mouli S, Hickey R, Kallini J, Gabr A, *et al*. Y90 radioembolization significantly prolongs time to progression compared with chemoembolization in patients with hepatocellular carcinoma. *Gastroenterology* 2016;151: 1155–1163. https://doi.org/10.1053/j.gastro.2016.08.029. e2.

[14] Van Cutsem E, Cervantes A, Adam R, Sobrero A, Van Krieken JH, Aderka D, *et al*. ESMO consensus guidelines for the management of patients with metastatic colorectal cancer. *Ann Oncol* 2016;27:1386–1422. https://doi.org/10.1093/annonc/mdw235.

[15] Kennedy A, Nag S, Salem R, Murthy R, McEwan AJ, Nutting C, *et al*. Recommendations for radioembolization of hepatic malignancies using yttrium-90 microsphere brachytherapy: a consensus panel report from the Radioembolization Brachytherapy Oncology Consortium. *Int J Radiat Oncol Biol Phys* 2007;68:13–23. https://doi.org/10.1016/j.ijrobp.2006.11.060.

[16] Salem R, Padia SA, Lam M, Bell J, Chiesa C, Fowers K, *et al*. Clinical and dosimetric considerations for Y90: recommendations from an international multidisciplinary working group. *Eur J Nucl Med Mol Imag* 2019;46:1695–1704. https://doi.org/10.1007/s00259-019-04340-5.

[17] Vogel A, Cervantes A, Chau I, Daniele B, Llovet JM, Meyer T, *et al*. Hepatocellular carcinoma: ESMO Clinical Practice Guidelines for diagnosis, treatment and follow-up. *Ann Oncol* 2019;29(Suppl 4):iv238–iv255. https://doi.org/10.1093/annonc/mdy308.

[18] Vilgrain V, Pereira H, Assenat E, Guiu B, Ilonca AD, Pageaux G-P, *et al*. Efficacy and safety of selective internal radiotherapy with yttrium-90 resin microspheres compared with sorafenib in locally advanced and inoperable hepatocellular carcinoma (SARAH): an open-label randomised controlled phase 3 trial. *Lancet Oncol* 2017;18:1624–1636. https://doi.org/10.1016/S1470-2045(17)30683-6.

[19] Ricke J, Bulla K, Kolligs F, Peck-Radosavljevic M, Reimer P, Sangro B, *et al*. Safety and toxicity of radioembolization plus Sorafenib in advanced hepatocellular carcinoma: analysis of the European multicentre trial SORAMIC. *Liver Int* 2015;35: 620–626. https://doi.org/10.1111/liv.12622.

[20] Chow PKH, Gandhi M, Tan SB, Khin MW, Khasbazar A, Ong J, *et al*. SIRveNIB: Selective internal radiation therapy versus sorafenib in Asia-Pacific patients with hepatocellular carcinoma. *J Clin Oncol* 2018;36:1913–1921. https://doi.org/10.1200/JCO.2017.76.0892.

[21] Sharma RA, Wasan HS, Van Hazel GA, Heinemann V, Sharma NK, Taieb J, *et al*. Overall survival analysis of the FOXFIRE prospective randomized studies of first-line selective internal radiotherapy (SIRT) in patients with liver metastases from colorectal cancer. *J Clin Oncol* 2017;35:3507. https://doi.org/10.1200/JCO.2017.35.15_suppl.3507.

[22] Gates VL, Singh N, Lewandowski RJ, Spies S, Salem R. Intraarterial hepatic SPECT/CT imaging using 99mTc-macroaggregated albumin in preparation for radioembolization. *J Nucl Med* 2015;56: 1157–1162. https://doi.org/10.2967/jnumed.114.153346.

[23] Powerski MJ, Erxleben C, Scheurig-Münkler C, Geisel D, Hamm B, Gebauer B. Anatomic variants of arteries often coil-occluded prior to hepatic radioembolization. *Acta Radiol* 2014;56:159–165. https://doi.org/10.1177/0284185114522148.

[24] Barentsz MW, Vente MAD, Lam MGEH, Smits MLJ, Nijsen JFW, Seinstra BA, *et al*. Technical solutions to ensure safe yttrium-90 radioembolization in patients with initial extrahepatic deposition of 99mtechnetium-albumin macroaggregates. *Cardiovasc Intervent Radiol* 2011;34:1074–1079. https://doi.org/10.1007/s00270-010-0088-4.

[25] Wright CL, Werner JD, Tran JM, Gates VL, Rikabi AA, Shah MH, *et al*. Radiation pneumonitis following yttrium-90 radioembolization: case report and literature review. *J Vasc Interv Radiol* 2012;23:669–674. https://doi.org/10.1016/j.jvir.2012.01.059.

[26] Gaba RC, Zivin SP, Dikopf MS, Parvinian A, Casadaban LC, Lu Y, *et al*. Characteristics of primary and secondary hepatic malignancies associated with hepatopulmonary shunting. *Radiology* 2014;271:602–612. https://doi.org/10.1148/radiol.14131969.

[27] Elschot M, Nijsen JFW, Lam MGEH, Smits MLJ, Prince JF, Viergever MA, *et al*. 99mTc-MAA overestimates the absorbed dose to the lungs in radioembolization: a quantitative evaluation in patients treated with 166Ho-microspheres. *Eur J Nucl Med Mol Imag* 2014;41:1965–1975. https://doi.org/10.1007/s00259-014-2784-9.

[28] Bastiaannet R, Kappadath SC, Kunnen B, Braat AJAT, Lam MGEH, de Jong HWAM. The physics of radioembolization. *EJNMMI Phys* 2018;5:22. https://doi.org/10.1186/s40658-018-0221-z.

[29] Kennedy AS, McNeillie P, Dezarn WA, Nutting C, Sangro B, Wertman D, *et al*. Treatment parameters and outcome in 680 treatments of internal radiation with resin 90Y-microspheres for unresectable hepatic tumors. *Int J Radiat Oncol Biol Phys* 2009;74:1494–1500. https://doi.org/10.1016/j.ijrobp.2008.10.005.

[30] Smits MLJ, Nijsen JFW, van den Bosch MAAJ, Lam MGEH, Vente MAD, Mali WPTM, *et al*. Holmium-166 radioembolisation in patients with unresectable, chemorefractory liver metastases (HEPAR trial): a phase 1, dose-escalation study. *Lancet Oncol* 2012;13:1025–1034. https://doi.org/10.1016/S1470-2045(12)70334-0.

[31] Lyman JT. Complication probability as assessed from dose-volume histograms. *Radiat Res Suppl* 1985;8:S13–S19.

[32] Dawson LA, Ten Haken RK. Partial volume tolerance of the liver to radiation. *Semin Radiat Oncol* 2005;15:279–283. https://doi.org/10.1016/j.semradonc.2005.04.005.

[33] Sze DY, Lam MGEH. Reply to "The limitations of theoretical dose modeling for yttrium-90 radioembolization. *J Vasc Interv Radiol* 2014;25:1147–1148. https://doi.org/10.1016/j.jvir.2014.04.004.

[34] Flux G, Bardies M, Chiesa C, Monsieurs M, Savolainen S, Strand S-E, *et al*. Clinical radionuclide therapy dosimetry: the quest for the "Holy Gray. *Eur J Nucl Med Mol Imag* 2007;34: 1699–1700. https://doi.org/10.1007/s00259-007-0471-9.

[35] Kao YH, Tan EH, Ng CE, Goh SW. Clinical implications of the body surface area method versus partition model dosimetry for yttrium-90 radioembolization using resin microspheres: a technical review. *Ann Nucl Med* 2011;25:455–461. https://doi.org/10.1007/s12149-011-0499-6.

[36] Lam MGEH, Louie JD, Abdelmaksoud MHK, Fisher GA, Cho-Phan CD, Sze DY. Limitations of body surface area–based activity calculation for radioembolization of hepatic metastases in colorectal cancer. *J Vasc Interv Radiol* 2014;25: 1085–1093. https://doi.org/10.1016/j.jvir.2013.11.018.

[37] Ho S, Lau WY, Leung TWT, Chan M, Ngar YK, Johnson PJ, *et al*. Partition model for estimating radiation doses from yttrium-90 microspheres in treating hepatic tumours. *Eur J Nucl Med* 1996;23:947–952. https://doi.org/10.1007/BF01084369.

[38] van den Hoven AF, Rosenbaum CENM, Elias SG, de Jong HWAM, Koopman M, Verkooijen HM, *et al*. Insights into the dose-response relationship of radioembolization with resin 90y-microspheres: a prospective cohort study in patients with colorectal cancer liver metastases. *J Nucl Med* 2016;57:1014–1019. https://doi.org/10.2967/jnumed.115.166942.

[39] van Roekel C, Bastiaannet R, Smits MLJJ, Bruijnen RC, Braat AJAT, de Jong HWAM, *et al*. Dose-effect relationships of holmium-166 radioembolization in colorectal cancer. *J Nucl Med* 2020;120:243832. https://doi.org/10.2967/jnumed.120.243832. jnumed.

[40] Bastiaannet R, van Roekel C, Smits MLJ, Elias SG, van Amsterdam WAC, Doan D, *et al*. First evidence for a dose-response relationship in patients treated with 166Ho radioembolization: a prospective study. *J Nucl Med* 2020;61:608–612. https://doi.org/10.2967/jnumed.119.232751.

[41] Wondergem M, Smits MLJ, Elschot M, de Jong HWAM, Verkooijen HM, van den Bosch MAAJ, *et al*. 99mTc-macroaggregated albumin poorly predicts the intrahepatic distribution of 90Y resin microspheres in hepatic radioembolization. *J Nucl Med* 2013;54:1294–1301. https://doi.org/10.2967/jnumed.112.117614.

[42] Jadoul A, Bernard C, Lovinfosse P, Gérard L, Lilet H, Cornet O, *et al*. Comparative dosimetry between 99mTc-MAA SPECT/CT and 90Y PET/CT in primary and metastatic liver tumors. *Eur J Nucl Med Mol Imag* 2020;47:828–837. https://doi.org/10.1007/s00259-019-04465-7.

[43] Gnesin S, Canetti L, Adib S, Cherbuin N, Silva Monteiro M, Bize P, *et al*. Partition model-based 99mTc-MAA SPECT/CT predictive dosimetry compared with 90Y TOF PET/CT post-treatment dosimetry in radioembolization of hepatocellular carcinoma: a quantitative agreement comparison. *J Nucl Med* 2016;57:1672–1678. https://doi.org/10.2967/jnumed.116.173104.

[44] Haste P, Tann M, Persohn S, LaRoche T, Aaron V, Mauxion T, *et al*. Correlation of technetium-99m macroaggregated albumin and yttrium-90 glass microsphere biodistribution in hepatocellular carcinoma: a retrospective review of pre-treatment single photon emission CT and posttreatment positron emission tomography/CT. *J Vasc Interv Radiol* 2017;28:722–730. https://doi.org/10.1016/j.jvir.2016.12.1221. e1.

[45] Chiesa C, Maccauro M. 166Ho microsphere scout dose for more accurate radioembolization treatment planning. *Eur J Nucl Med Mol Imag* 2020;47:744–747. https://doi.org/10.1007/s00259-019-04617-9.

[46] Knešaurek K, Machac J, Muzinic M, DaCosta M, Zhang Z, Heiba S. Quantitative comparison of yttrium-90 (90 Y)-microspheres and technetium-99m (99m Tc)-macroaggregated albumin SPECT images for planning 90 Y therapy of liver cancer. *Technol Cancer Res Treat* 2010;9:253–261. https://doi.org/10.1177/153303461000900304.

[47] Jiang M, Fischman A, Nowakowski FS. Segmental perfusion differences on paired Tc-99m macroaggregated albumin (MAA) hepatic perfusion imaging and yttrium-90 (Y-90) bremsstrahlung imaging studies in SIR-sphere radioembolization: associations with angiography. *J Nucl Med Radiat Ther* 2012;3:1. https://doi.org/10.4172/2155-9619.1000122.

[48] Chiesa C, Mira M, De Nile MC, Maccauro M, Spreafico C, Zanette C, *et al*. Discrepancy between 99mTc-MAA SPECT and 90Y glass microspheres PET lung dosimetry in radioembolization of hepatocarcinoma. *Eur J Nucl Med Mol Imag* 2016;43:406. https://doi.org/10.1007/s00259-016-3484-4.

[49] Smits MLJ, Dassen MG, Prince JF, Braat AJAT, Beijst C, Bruijnen RCG, *et al*. The superior predictive value of 166Ho-scout compared with 99mTc-macroaggregated albumin prior to 166Ho-microspheres radioembolization in patients with liver metastases. *Eur J Nucl Med Mol Imag* 2020;47:798–806. https://doi.org/10.1007/s00259-019-04460-y.

[50] Bourgeois AC, Chang TT, Bradley YC, Acuff SN, Pasciak AS. Intraprocedural yttrium-90 positron emission tomography/CT for treatment optimization of yttrium-90 radioembolization. *J Vasc Interv Radiol* 2013;25:271–275. https://doi.org/10.1016/j.jvir.2013.11.004.

[51] Garin E, Rolland Y, Pracht M, Le Sourd S, Laffont S, Mesbah H, *et al*. High impact of macroaggregated albumin-based tumour dose on response and overall survival in hepatocellular carcinoma patients treated with 90 Y-loaded glass microsphere radioembolization. *Liver Int* 2017;37:101–110. https://doi.org/10.1111/liv.13220.

[52] Braat AJAT, Smits MLJ, Braat MNGJA, van den Hoven AF, Prince JF, de Jong HWAM, *et al*. 90Y hepatic radioembolization: an update on current practice and recent developments. *J Nucl Med* 2015;56:1079–1087. https://doi.org/10.2967/jnumed.115.157446.

[53] Brose MS, Frenette CT, Keefe SM, Stein SM. Management of sorafenib-related adverse events: a clinician's perspective. *Semin Oncol* 2014;41:S1–S16. https://doi.org/10.1053/j.seminoncol.2014.01.001.

[54] Braat MNGJA, van Erpecum KJ, Zonnenberg BA, van den Bosch MAJ, Lam MGEH. Radioembolization-induced liver disease: a systematic review. *Eur J Gastroenterol Hepatol* 2017;29:144–152. https://doi.org/10.1097/MEG.0000000000000772.

[55] Strigari L, Sciuto R, Rea S, Carpanese L, Pizzi G, Soriani A, *et al*. Efficacy and toxicity related to treatment of hepatocellular carcinoma with 90Y-SIR spheres: radiobiologic considerations. *J Nucl Med* 2010;51:1377–1385. https://doi.org/10.2967/jnumed.110.075861.

[56] Chiesa C, Mira M, Maccauro M, Spreafico C, Romito R, Morosi C, *et al*. Radioembolization of hepatocarcinoma with 90Y glass microspheres: development of an individualized treatment planning strategy based on dosimetry and radiobiology. *Eur J Nucl Med Mol Imag* 2015;42:1718–1738. https://doi.org/10.1007/s00259-015-3068-8.

[57] Gil-Alzugaray B, Chopitea A, Iñarrairaegui M, Bilbao JI, Rodriguez-Fraile M, Rodriguez J, *et al*. Prognostic factors and prevention of radioembolization-induced liver disease. *Hepatology* 2013;57:1078–1087. https://doi.org/10.1002/hep.26191.

[58] Chiesa C, Mira M, Bhoori S, Bormolini G, Maccauro M, Spreafico C, *et al*. Radioembolization of hepatocarcinoma with 90Y glass microspheres: treatment optimization using the dose-toxicity relationship. *Eur J Nucl Med Mol Imag* 2020;47:3018–3032. https://doi.org/10.1007/s00259-020-04845-4.

[59] Cremonesi M, Chiesa C, Strigari L, Ferrari M, Botta F, Guerriero F, *et al*. Radioembolization of hepatic lesions from a radiobiology and dosimetric perspective. *Front Oncol* 2014;4:210. https://doi.org/10.3389/fonc.2014.00210.

[60] Chan KT, Alessio AM, Johnson GE, Vaidya S, Kwan SW, Monsky W, *et al*. Prospective trial using internal pair-production positron emission tomography to establish the yttrium-90 radioembolization dose required for response of hepatocellular carcinoma. *Int J Radiat Oncol Biol Phys* 2018;101:358–365. https://doi.org/10.1016/j.ijrobp.2018.01.116.

[61] Chiesa C. The individualized dosimetry in the radioembolization of hepatocarcinoma with 90Y-microspheres.

*Phys Med* 2016;32:169–170. https://doi.org/10.1016/j.ejmp.2016.07.264.

[62] Hermann A-L, Dieudonné A, Ronot M, Sanchez M, Pereira H, Chatellier G, *et al*. Relationship of tumor radiation–absorbed dose to survival and response in hepatocellular carcinoma treated with transarterial radioembolization with 90 Y in the SARAH study. *Radiology* 2020;296:673–684. https://doi.org/10.1148/radiol.2020191606.

[63] Kafrouni M, Allimant C, Fourcade M, Vauclin S, Guiu B, Mariano-Goulart D, *et al*. Analysis of differences between 99mTc-MAA SPECT- and 90Y-microsphere PET-based dosimetry for hepatocellular carcinoma selective internal radiation therapy. *EJNMMI Res* 2019;9:62. https://doi.org/10.1186/s13550-019-0533-6.

[64] Garin E, Tselikas L, Guiu B, Chalaye J, Edeline J, de Baere T, *et al*. Personalised versus standard dosimetry approach of selective internal radiation therapy in patients with locally advanced hepatocellular carcinoma (DOSISPHERE-01): a randomised, multicentre, open-label phase 2 trial. *Lancet Gastroenterol Hepatol* 2020;1253:1–13. https://doi.org/10.1016/S2468-1253(20)30290-9.

[65] Alsultan AA, van Roekel C, Barentsz MW, Smits MLJ, Kunnen B, Koopman M, *et al*. Dose-response relationship in glass yttrium-90 microsphere radioembolization in patients with colorectal cancer liver metastases [Abstract]. *Cardiovasc Intervent Radiol* 2020;43:164. https://doi.org/10.1007/s00270-020-02606-2.

[66] Wasan HS, Gibbs P, Sharma NK, Taieb J, Heinemann V, Ricke J, *et al*. First-line selective internal radiotherapy plus chemotherapy versus chemotherapy alone in patients with liver metastases from colorectal cancer (FOXFIRE, SIRFLOX, and FOXFIRE-Global): a combined analysis of three multicentre, randomised, phase 3 trials. *Lancet Oncol* 2017;18:1159–1171. https://doi.org/10.1016/S1470-2045(17)30457-6.

[67] Chauhan N, Mulcahy MF, Salem R, Benson AB, Boucher E, Bukovcan J, *et al*. Therasphere yttrium-90 glass microspheres combined with chemotherapy versus chemotherapy alone in second-line treatment of patients with metastatic colorectal carcinoma of the liver: protocol for the EPOCH phase 3 randomized clinical trial. *J Med Internet Res* 2019;8:e11545. https://doi.org/10.2196/11545.

[68] Sposito C, Mazzaferro V. The SIRveNIB and SARAH trials, radioembolization vs. sorafenib in advanced HCC patients: reasons for a failure, and perspectives for the future. *HepatoBiliar Surg Nutr* 2018;7:487–489. https://doi.org/10.21037/hbsn.2018.10.06.

[69] Kao YH, Steinberg JD, Tay YS, Lim GKY, Yan J, Townsend DW, *et al*. Post-radioembolization yttrium-90 PET/CT-part 2: Dose-response and tumor predictive dosimetry for resin microspheres. *EJNMMI Res* 2013;3:1–27. https://doi.org/10.1186/2191-219X-3-57.

[70] Chiesa C, Bardiès M, Zaidi H. Voxel-based dosimetry is superior to mean absorbed dose approach for establishing dose-effect relationship in targeted radionuclide therapy. *Med Phys* 2019;46:5403–5406. https://doi.org/10.1002/mp.13851.

[71] Beijst C, Elschot M, Viergever MA, de Jong HWAM. Toward simultaneous real-time fluoroscopic and nuclear imaging in the intervention room. *Radiology* 2016;278:232–238. https://doi.org/10.1148/radiol.2015142749.

[72] van der Velden S, Kunnen B, Koppert WJC, Steenbergen JHL, Dietze MMA, Beijst C, *et al*. A dual-layer detector for simultaneous fluoroscopic and nuclear imaging. *Radiology* 2019;290:833–838. https://doi.org/10.1148/radiol.2018180796.